LETTER

doi:10.1038/nature11748

Suppression of neuroinflammation by astrocytic dopamine D2 receptors via αB-crystallin

Wei Shao[1]*, Shu-zhen Zhang[1]*, Mi Tang[1,2], Xin-hua Zhang[1], Zheng Zhou[1], Yan-qing Yin[1], Qin-bo Zhou[1], Yuan-yuan Huang[1], Ying-jun Liu[1], Eric Wawrousek[3], Teng Chen[4], Sheng-bin Li[4], Ming Xu[5], Jiang-ning Zhou[6], Gang Hu[2] & Jia-wei Zhou[1]

Chronic neuroinflammation is a common feature of the ageing brain and some neurodegenerative disorders. However, the molecular and cellular mechanisms underlying the regulation of innate immunity in the central nervous system remain elusive. Here we show that the astrocytic dopamine D2 receptor (DRD2) modulates innate immunity through αB-crystallin (CRYAB), which is known to suppress neuroinflammation[1,2]. We demonstrate that knockout mice lacking *Drd2* showed remarkable inflammatory response in multiple central nervous system regions and increased the vulnerability of nigral dopaminergic neurons to neurotoxin 1-methyl-4-phenyl-1,2,3,6-tetrahydropyridine (MPTP)-induced neurotoxicity[3]. Astrocytes null for *Drd2* became hyper-responsive to immune stimuli with a marked reduction in the level of CRYAB. Preferential ablation of *Drd2* in astrocytes robustly activated astrocytes in the substantia nigra. Gain- or loss-of-function studies showed that CRYAB is critical for DRD2-mediated modulation of innate immune response in astrocytes. Furthermore, treatment of wild-type mice with the selective DRD2 agonist quinpirole increased resistance of the nigral dopaminergic neurons to MPTP through partial suppression of inflammation. Our study indicates that astrocytic DRD2 activation normally suppresses neuroinflammation in the central nervous system through a CRYAB-dependent mechanism, and provides a new strategy for targeting the astrocyte-mediated innate immune response in the central nervous system during ageing and disease.

Neuroglial cells are essential for the maintenance of brain homeostasis. Activated neuroglial cells contribute to immune deregulation and neuroinflammation, which are associated with ageing and a variety of neurodegenerative disorders[4]. The ageing of the human brain and progression of cognitive and motor function impairment in the elderly are accompanied with downregulation of DRD2 density in both the striatum and several extrastriatal regions in the normal brain[5–7]. Recent data indicate that full sets of neurotransmitter receptors, including dopamine receptors, are expressed in microglia and astrocytes[8–10]. Therefore, we asked whether the deficits in glial DRD2 signalling affect the innate immune response contributing to unbalanced brain homeostasis and disease progression.

To unravel the potential role of DRD2 in neuroinflammation, we examined the expression of an astroglial marker, glial fibrillary acid protein (GFAP) and a microglial marker, ionized calcium binding adaptor molecule 1 (IBA1) in global *Drd2*-knockout ($Drd2^{-/-}$) mice and their wild-type counterparts using immunohistochemistry. In young (2-month-old) *Drd2*-deficient mice, there was pronounced activation of astrocytes (~160%) in the substantia nigra (Fig. 1a, b). In old *Drd2*-null mice (16-month-old), the astrogliosis in the substantia nigra and striatum were also more severe than in age- and gender-matched wild-type mice (Supplementary Fig. 2). Comparatively more microglial reactivity was seen in these animals (Fig. 1a, c and Supplementary Fig. 2a). To determine whether the *Drd2*-depletion-induced activation of glial cells contribute to neurodegeneration of nigral dopaminergic neurons, $Drd2^{-/-}$ mice were treated with neurotoxin 1-methyl-4-phenyl-1,2,3,6-tetrahydropyridine (MPTP). This resulted in more severe loss of nigral dopaminergic neurons compared with their wild-type counterparts (Fig. 1d, e). This difference was associated with more severe inflammation in these brain regions of $Drd2^{-/-}$ mice (Fig. 1a–c).

Further biochemical analysis showed that the enhanced vulnerability of nigral dopaminergic neurons was associated with aberrant expression of inflammatory mediators. In 2-month-old $Drd2^{-/-}$ mice, there were pronounced increases in levels of CD68, an inflammatory protein expressed in macrophage/microglia, and interleukin (IL)-1β in various regions of the central nervous system, but not in the immune organ thymus (Fig. 1f and Supplementary Fig. 3a). Quantitative PCR (qPCR) analysis revealed that the expression of pro-inflammatory mediator genes, including *IL-1β*, *IL-2*, *IL-6*, *IL-12β*, cyclooxygenase-2 (*COX-2*; genes also known as *Il1b*, *Il2*, *Il6*, *Il12b* and *Ptgs2*, respectively), and anti-inflammatory cytokine *IL-10* (also known as *Il10*), but not tumour necrosis factor-α (*TNF-α*, also known as *Tnfa*), were significantly increased in the striatum of *Drd2*-null mice compared to wild-type mice (Fig. 1g). Moreover, advanced age exacerbates inflammation (Supplementary Fig. 3b). In contrast, ablation of other dopamine receptor subtypes *Drd1* or *Drd3* only resulted in mild or no significant alteration in the levels of pro-inflammatory mediators in the central nervous system (Supplementary Figs 4 and 5). These data indicate that the absence of *Drd2* tipped the balance of cell signalling network towards activation of inflammatory genes in organ-specific and age-dependent manners.

To define the cell types responsible for *Drd2*-ablation-mediated inflammation, we assessed the levels of inflammatory mediators under basal conditions *in vitro*. Expression of major inflammatory mediators were not significantly altered in microglia and neurons isolated from *Drd2*-null pups compared to wild-type control (Fig. 2a and data not shown). In contrast, *Drd2*-null astrocytes produced more pro-inflammatory agents than their wild-type counterparts (Fig. 2b and Supplementary Fig. 6a–d). Interestingly, *Drd2*-null astrocytes and microglia showed a distinctive response to immune stimuli. Astrocytes null for *Drd2* showed a marked increase in the levels of pro-inflammatory mediators, but not NURR1[11], compared with wild-type astrocytes following exposure to the conditioned medium of toll-like receptor ligands lipopolysaccharide (LPS)-treated microglia (Fig. 2b and Supplementary Figs 6c, d and 7), indicating that *Drd2*-null astrocytes were hyper-responsive. Conversely, microglia from null

[1]Institute of Neuroscience, State Key Laboratory of Neuroscience, Shanghai Institutes for Biological Sciences, Chinese Academy of Sciences, Shanghai 200031, China. [2]Jiangsu Key Laboratory of Neurodegeneration, Department of Pharmacology, Nanjing Medical University, Nanjing, Jiangsu 210029, China. [3]National Eye Institute, NIH, Bethesda, Maryland 20892, USA. [4]Department of Forensic Science, Xi'an Jiaotong University School of Medicine, Xi'an, Shanxi 710061, China. [5]Department of Anesthesia and Critical Care, University of Chicago, Chicago, Illinois 60637, USA. [6]CAS Key Laboratory of Brain Function and Diseases, School of Life Science, University of Science and Technology of China, Hefei, Anhui 230027, China.
*These authors contributed equally to this work.

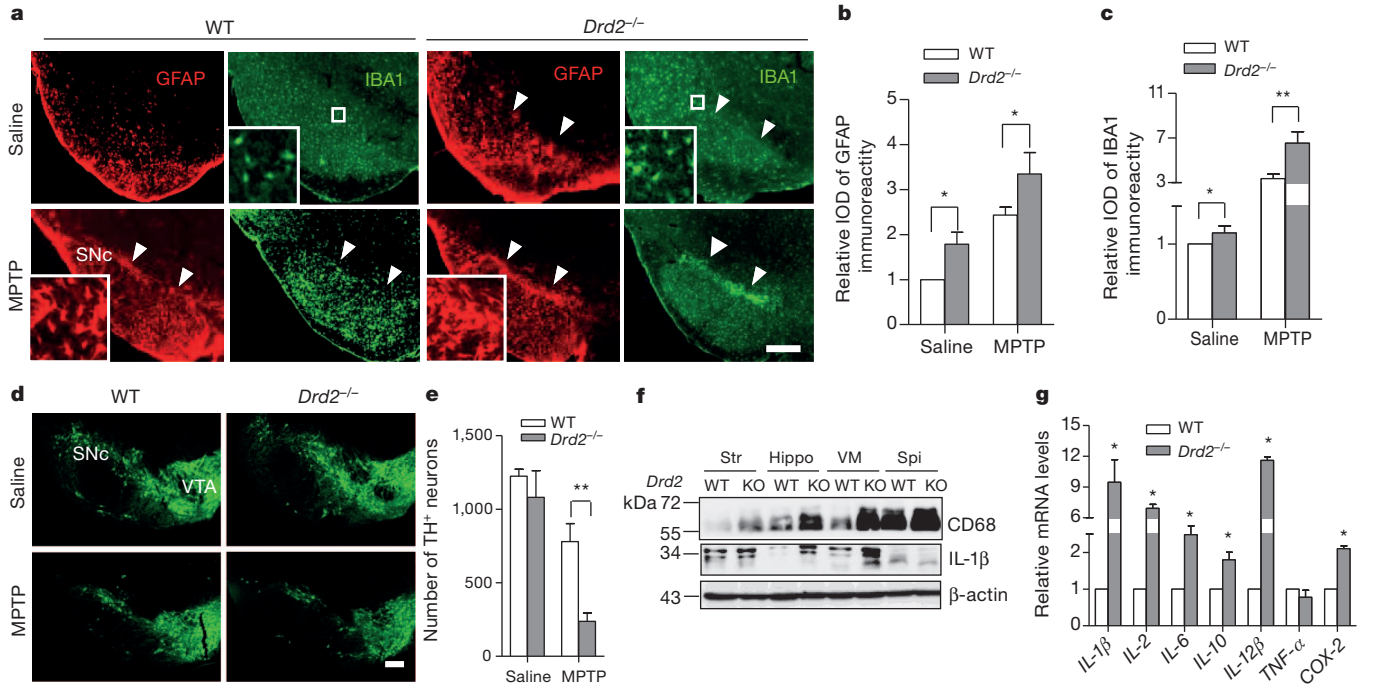

Figure 1 | More severe activation of astrocytes and microglia and pronounced inflammatory responses in global *Drd2*-deficient mice. **a**–**e**, Immunofluorescent histochemical staining for GFAP, IBA1 and tyrosine hydroxylase (TH) on the ventral mesencephalon of 2-month-old wild-type (WT) and $Drd2^{-/-}$ mice administrated with either saline or MPTP (**a**, **d**) and quantitative data (**b**, **c**, **e**) are shown. Inserts are enlarged views of the substantia nigra pars compacta (SNc) of the corresponding photo. Arrow heads indicate the SNc. Scale bar, 500 μm. Data are expressed as mean ± s.e.m. (**b**, $n = 10$ per group; **c**, **e**, $n = 6$ per group); $^{*}P < 0.05$; $^{**}P < 0.01$ compared to control. IOD, integrated optical density. **f**, Representative western blots from two separate experiments showing CD68 and IL-1β expression in the various brain regions from 2-month-old WT and global $Drd2^{-/-}$ mice. Hippo, hippocampus; Spi, spinal cord; Str, striatum; VM, ventral mesencephalon. **g**, Representative graph showing relative mRNA levels of inflammatory mediators in the striatum from WT and global $Drd2^{-/-}$ mice. Data are expressed as mean ± s.e.m. ($n = 4$), $^{*}P < 0.05$ compared to control.

animals did not show a similar hyper-responsiveness when stimulated in culture with LPS (Fig. 2a). Furthermore, co-culture of mesencephalic dopaminergic neurons with *Drd2*-null astrocytes resulted in a significantly reduced survival of tyrosine-hydroxylase-positive neurons (Supplementary Fig. 6e).

To determine whether *Drd2*-deficiency-induced neuroinflammation occurs at the level of the substantia nigra in a non-cell autonomous fashion, we crossed $Drd2^{flox/flox}$ mice with human GFAP (hGFAP)-Cre recombinase transgene[12] to generate *Drd2* conditional knockout mice, $Drd2^{flox/flox}$; *hGFAP-Cre* (hereafter referred to as $Drd2^{hGFAP}$ *cKO*) in which *Drd2* is preferentially inactivated in astrocytes. Remarkable loss of *Drd2* messenger RNA was observed in cultured astrocytes, whereas no marked excision in striatal tissue was detected by qPCR analysis (Supplementary Fig. 8a, b), indicating that astrocytic DRD2 is of very low abundance in overall levels of DRD2 in the striatal tissue. In young knockout progeny at postnatal day (P) 10–16, mesencephalic dopaminergic neuron development was normal (Supplementary Fig. 8c, d). With advancing age, mesencephalic dopaminergic neurons were maintained, whereas the levels of inflammatory mediators in the substantia nigra of $Drd2^{hGFAP}$ *cKO* mice were remarkably elevated (Fig. 2c, d), which is in accordance with Fig. 1a. $Drd2^{hGFAP}$ *cKO* mice treated with MPTP showed no marked alteration in cell proliferation in the substantia nigra (Supplementary Fig. 9). The ventral tegmental area (VTA) was essentially devoid of activated glial cells (Supplementary Fig. 10). Selective deletion of *Drd2* in neuronal cells *in vivo* resulted in very mild increases in the levels of pro-inflammatory mediators (Supplementary Fig. 11). Taken together, these data indicate that astrocytic DRD2 is a key negative regulator for neuroinflammation.

To identify downstream effectors of *Drd2* that might be responsible for regulating inflammatory mediator production, DNA microarray analysis was carried out to compare striatal gene transcript profiles between *Drd2*-null mice and their wild-type littermates. Reduction of αB-crystallin (CRYAB) was prominently detected in *Drd2*-null mice compared to wild-type counterparts (Supplementary Table 1 and Supplementary Fig. 12a). CRYAB is known as a small heat-shock protein with anti-inflammatory and neuroprotective activities[1,2]. In the brain it is expressed primarily in astrocytes and oligodendrocytes[2,13,14]. Ablation of *Drd2*, but not *Drd1*, resulted in remarkable reduction of CRYAB exclusively in the central nervous system (Supplementary Fig. 12b–f). Furthermore, we found that in either primary cultured astrocytes null for *Drd2* or the central nervous system tissue of $Drd2^{hGFAP}$ *cKO* mice and tamoxifen (TAM)-inducible $Drd2^{hGFAP}$ *cKO* mice, there was pronounced reduction of CRYAB compared to control animals (Fig. 3a and Supplementary Figs 8a, b and 12a, g, h). These analyses indicate that astrocytic DRD2 tightly controls CRYAB expression in astrocytes. Interestingly, some components of classical DRD2 signalling probably contributed to the inflammatory response because the TAM-inducible $Drd2^{hGFAP}$ *cKO* mice displayed enhanced phosphorylated levels of GSK3β(Ser 9), GSK3β(Tyr 216) and p44/42 MAPK (Thr 202/Tyr 204) in the striatum (Supplementary Fig. 13).

To unravel the role of CRYAB on inflammatory mediator expression in astrocytes, we evaluated the impact of altering CRYAB expression. Small interfering RNA knockdown of *Cryab* in cultured astrocytes markedly upregulated pro-inflammatory mediators compared to control (Supplementary Fig. 14a–c). In the substantia nigra of adult *Cryab*-null mice, astrocytes were robustly activated, showing intense GFAP immunoreactivity, but no marked dopaminergic neuron loss in this brain region (Supplementary Fig. 15). Moreover, overexpression of Flag-tagged CRYAB in cultured *Drd2*-null astrocytes resulted in a marked reduction in the levels of

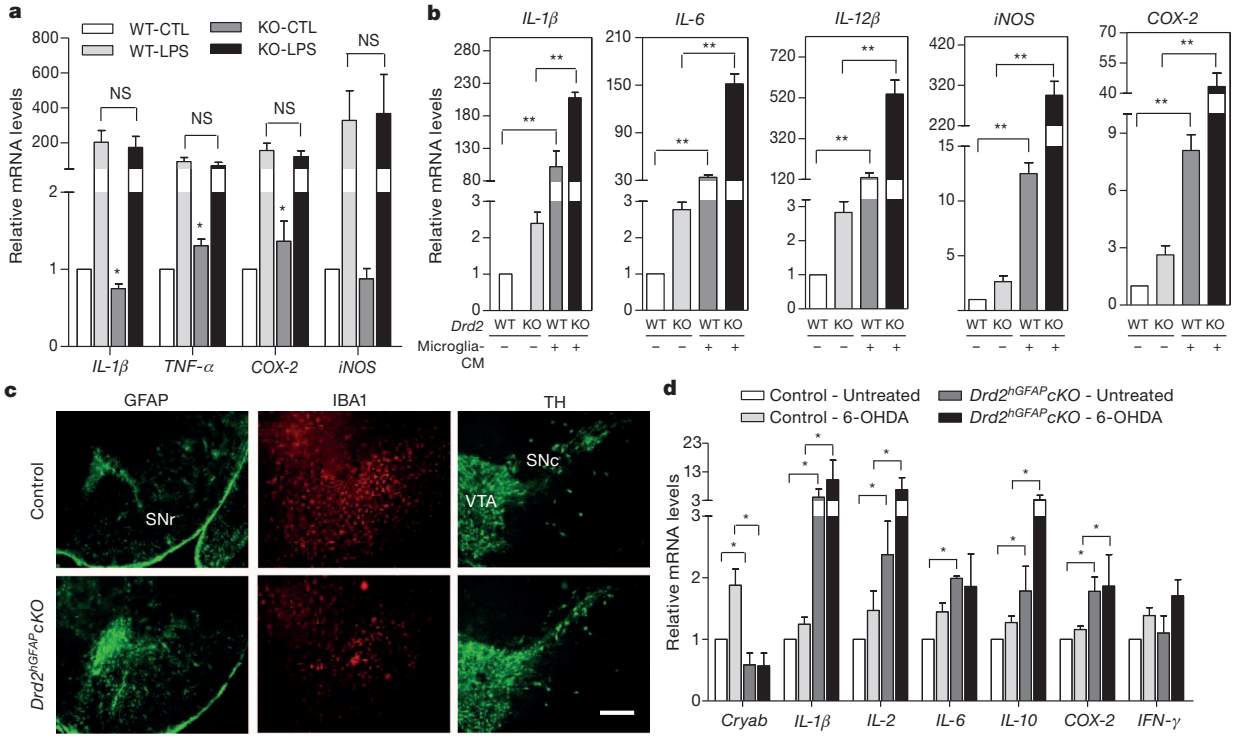

Figure 2 | Astrocytes from global *Drd2*$^{-/-}$ mice are hyper-responsive. **a**, Representative graph showing relative mRNA levels of the indicated pro-inflammatory mediators from primary cultured microglia isolated from WT and global *Drd2*$^{-/-}$ mice and stimulated with lipopolysaccharide (LPS). Data are expressed as mean ± s.e.m. ($n = 10$); $^{*}P < 0.05$; $^{**}P < 0.01$ compared to WT control. CTL, control; NS, not significant. **b**, Representative graph showing relative mRNA levels of *IL-1β*, *IL-6*, *IL-12β*, iNOS (also known as *Nos2*) and *COX-2* from primary cultured astrocytes isolated from WT and global *Drd2*$^{-/-}$ mice and stimulated with the conditioned medium of microglia treated with LPS for 24 h. **c**, Immunofluorescent histochemical staining for GFAP, IBA1 and TH on the ventral mesencephalon of 3-week-old *Drd2*^{hGFAP} *cKO* mice compared with control. SNr, substantia nigra pars reticulata. Scale bar, 200 μm. **d**, Representative graph showing relative mRNA levels of *Cryab* and pro/anti-inflammatory mediators in 2-month-old *Drd2*^{hGFAP} *cKO* and control (*Drd2*$^{+/+}$;*hGFAP-Cre*$^{+}$) animals treated with or without 6-hydroxydopamine (6-OHDA). Data are expressed as mean ± s.e.m. ($n = 3$); $^{*}P < 0.05$.

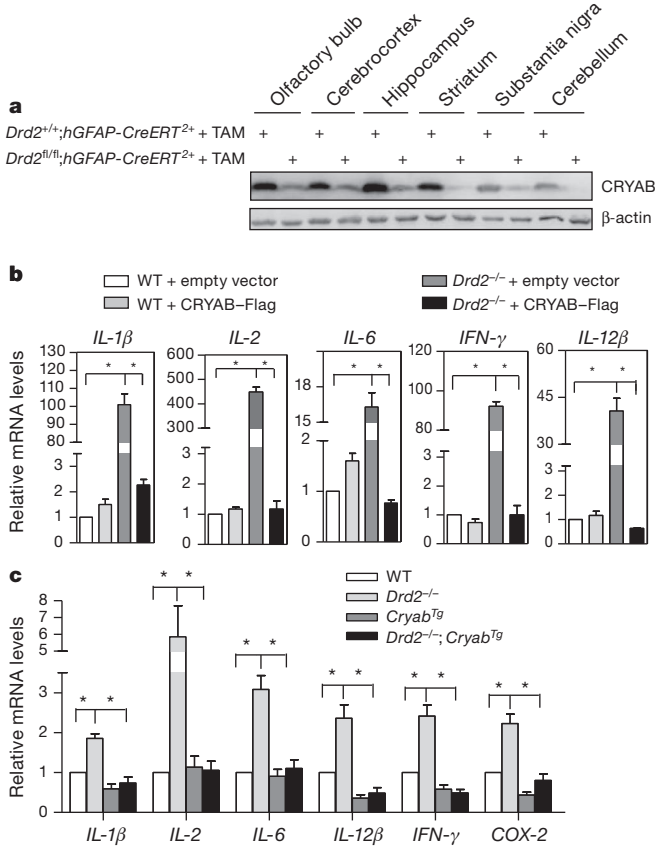

pro-inflammatory mediators compared to control (Fig. 3b and Supplementary Fig. 14d–f). Furthermore, we crossed transgenic mice expressing the hamster *Cryab* gene under the control of hGFAP promoter to target expression to astrocytes (hereafter referred to as CRYAB^{Tg})[14] with global *Drd2*$^{-/-}$ mice. Overexpression of CRYAB remarkably inhibited the aberrant increase of pro-inflammatory mediators in the *Drd2*$^{-/-}$ mice (Fig. 3c and Supplementary Fig. 14g). Together, these results indicate that CRYAB is required for *Drd2*-mediated suppression of inflammatory response in astrocytes. To investigate the physiological relevance of these findings, we examined expression of CRYAB in a MPTP-induced mouse model of Parkinson's disease[15]. We found intense CRYAB immunosignals in the substantia nigra and striatum of MPTP-treated wild-type mice, some of which were confined to reactive astrocytes (Supplementary Fig. 16).

To determine whether DRD2 signalling is required for suppression of inflammatory response *in vivo*, wild-type mice were treated with

Figure 3 | CRYAB overexpression suppresses *Drd2* deficiency-induced inflammation. **a**, Preferential depletion of *Drd2* in astrocytes results in marked reduction of CRYAB in the central nervous system. Western blot analysis of tissue lysates from the indicated central nervous system regions of 5-month-old inducible conditional *Drd2* knockout mice treated with tamoxifen (TAM). **b**, Transcript levels of the indicated genes evaluated in CRYAB-overexpressing *Drd2*-null astrocytes exposed to the conditioned medium from LPS-treated microglia by qPCR. Data are expressed as mean ± s.e.m. ($n = 3$); $^{*}P < 0.05$. **c**, CRYAB overexpression specifically targeting astrocytes suppresses the *Drd2*-deficiency-induced aberrant expression of the indicated inflammatory mediators in the striatum *in vivo* as shown by qPCR.

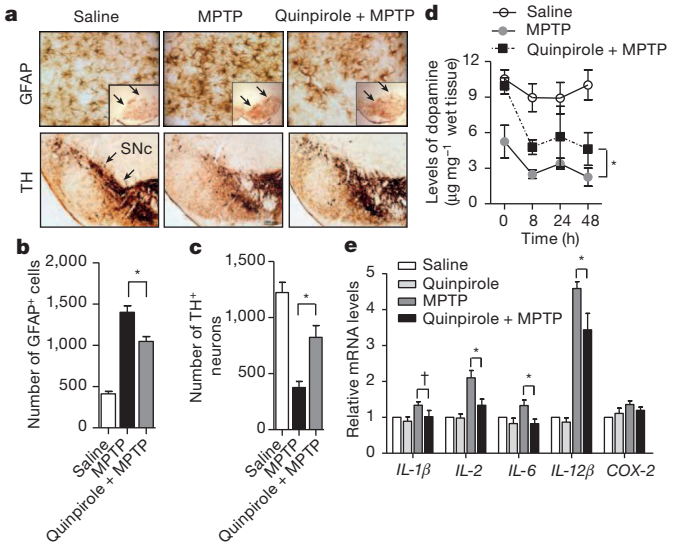

Figure 4 | *In vivo* activation of DRD2 inhibits astrogliosis and inflammation elicited by MPTP treatment. **a**–**c**, Immunohistochemical analysis of the ventral mesencephalon sections taken after 7 days from wild-type mice that received repeated quinpirole and MPTP administration. **b**, **c**, Quantitative data shown in **a**. Data are expressed as mean ± s.e.m. ($n = 6$); $^*P < 0.05$. Scale bar, 200 μm. **d**, Measurement of striatal dopamine levels were performed in wild-type mice pretreated with quinpirole before MPTP treatment at various times (0, 8, 24, 48 h). Data are expressed as mean ± s.e.m. ($n = 6$); $^*P < 0.05$. **e**, Transcript levels of the indicated genes evaluated in the striatum of wild-type mice treated with quinpirole or MPTP alone at 56 h after initial MPTP injection. Data are expressed as mean ± s.e.m. ($n = 6$); $\dagger P = 0.058$, $^*P < 0.05$.

quinpirole before MPTP administration (Supplementary Fig. 17a). Repeated quinpirole administration resulted in a marked reduction in the level of activation of astrocytes and microglia in the nigrostriatal pathway compared to control (Fig. 4a, b and Supplementary Fig. 17b, c, e, f). As expected, activation of DRD2 significantly prevented the MPTP-induced loss of nigral dopaminergic neurons and their terminals in the striatum (Fig. 4a, c and Supplementary Fig. 17b, d). Consistent with these results, quinpirole significantly attenuated the acute decrease of striatal dopaminergic levels, as shown by high-performance liquid chromatography (HPLC) measurement, and reduced the levels of pro-inflammatory mediators in the substantia nigra of MPTP-treated mice compared with the mice treated with MPTP alone (Fig. 4d, e). In contrast, *Drd2*-null mice as well as *Cryab*-null mice failed to show attenuation of astrocyte activation in the nigrostriatal pathway induced either by MPTP or 6-hydroxydopamine following quinpirole treatment, respectively (Supplementary Figs 18 and 19). Our data indicate that the use of a DRD2 agonist reduced the severity of the neuroinflammatory response when administered before MPTP.

Our results identify astrocytic DRD2 as an important component of neural network controlling innate immunity in the central nervous system. Astrocytic *Drd2* tightly controls the expression of CRYAB which accounts for the observed modulation of immune balance. By influencing CRYAB expression, DRD2 may modulate inflammatory response and maintain balance of immune state, representing a completely novel function in the central nervous system (Supplementary Fig. 1). Microglia has long been considered a key player in neuroinflammation[11,16–18]. However, our data indicate that astrocytes are likely to play a previously unexpected but critical function in the modulation of neuroinflammation in the context of *Drd2* deficiency. These findings open up new avenues in the investigation of brain ageing and neuroinflammation-associated central nervous system disorders.

METHODS SUMMARY

Adult or neonatal C57BL/6 mice were from Shanghai Laboratory Animal Center, Chinese Academy of Sciences. *Drd2* (B6.129S2-*Drd2*^{tm1Low}/J), *Drd1* (B6.129S4-*Drd1a*^{tm1Jcd}/J) heterozygous mice and *Cryab* transgenic mice (FVB-Tg(GFAP-CRYAB)141.6Mes/J) were purchased from the Jackson Laboratory. *Drd2*$^{-/-}$ mice in a C57BL/6 (inbred) genetic background generated by 10 backcrosses were used in the entire study. *Drd2*-floxed mice were created by Shanghai Research Center for Model Organisms. *Cryab* and *Drd3* mutant mice in 129/Sv genetic background used in this study were characterized previously[2,19,20]. hGFAP-Cre transgenic mice in a C57BL/6 genetic background, which was originally derived from FVB-Tg(GFAP-Cre)25Mes/J (Jackson Laboratory), were gifts from S. M. Duan. hGFAP-CreER^{T2} transgenic mice in a C57BL/6 genetic background were kindly provided by K. D. McCarthy[21]. Neuron-specific enolase (*NSE*)-Cre transgenic mice in a C57BL/6 genetic background were gifts from J. Fei. Genotyping was performed as previously described[22]. Western blotting, primary cell culture, immunohistochemistry, fluorescence intensity measurements, Affymetrix microarray analysis, qPCR and statistics were performed as described in Methods.

Full Methods and any associated references are available in the online version of the paper.

Received 1 August 2011; accepted 7 November 2012.
Published online 16 December 2012.

1. Bhat, R. & Steinman, L. Innate and adaptive autoimmunity directed to the central nervous system. *Neuron* **64,** 123–132 (2009).
2. Ousman, S. S. *et al.* Protective and therapeutic role for αB-crystallin in autoimmune demyelination. *Nature* **448,** 474–479 (2007).
3. Langston, J. W., Ballard, P., Tetrud, J. W. & Irwin, I. Chronic Parkinsonism in humans due to a product of meperidine-analog synthesis. *Science* **219,** 979–980 (1983).
4. Lucin, K. M. & Wyss-Coray, T. Immune activation in brain aging and neurodegeneration: too much or too little? *Neuron* **64,** 110–122 (2009).
5. Seeman, P. *et al.* Human brain dopamine receptors in children and aging adults. *Synapse* **1,** 399–404 (1987).
6. Kaasinen, V. *et al.* Age-related dopamine D2/D3 receptor loss in extrastriatal regions of the human brain. *Neurobiol. Aging* **21,** 683–688 (2000).
7. Antonini, A. & Leenders, K. L. Dopamine D2 receptors in normal human brain: effect of age measured by positron emission tomography (PET) and [^{11}C]-raclopride. *Ann. NY Acad. Sci.* **695,** 81–85 (1993).
8. Zhang, Y. & Barres, B. A. Astrocyte heterogeneity: an underappreciated topic in neurobiology. *Curr. Opin. Neurobiol.* **20,** 588–594 (2010).
9. Bal, A. *et al.* Evidence for D_2 receptor mRNA expression by striatal astrocytes in culture: in situ hybridization and polymerase chain reaction studies. *Brain Res. Mol. Brain Res.* **23,** 204–212 (1994).
10. Luo, X., Zhang, X., Shao, W., Yin, Y. & Zhou, J. Crucial roles of MZF-1 in the transcriptional regulation of apomorphine-induced modulation of FGF-2 expression in astrocytic cultures. *J. Neurochem.* **108,** 952–961 (2009).
11. Saijo, K. *et al.* A Nurr1/CoREST pathway in microglia and astrocytes protects dopaminergic neurons from inflammation-induced death. *Cell* **137,** 47–59 (2009).
12. Zhuo, L. *et al.* hGFAP-cre transgenic mice for manipulation of glial and neuronal function *in vivo*. *Genesis* **31,** 85–94 (2001).
13. Iwaki, T., Kume-Iwaki, A., Liem, R. K. & Goldman, J. E. αB-crystallin is expressed in non-lenticular tissues and accumulates in Alexander's disease brain. *Cell* **57,** 71–78 (1989).
14. Hagemann, T. L., Boelens, W. C., Wawrousek, E. F. & Messing, A. Suppression of GFAP toxicity by αB-crystallin in mouse models of Alexander disease. *Hum. Mol. Genet.* **18,** 1190–1199 (2009).
15. Jackson-Lewis, V. & Przedborski, S. Protocol for the MPTP mouse model of Parkinson's disease. *Nature Protocols* **2,** 141–151 (2007).
16. Rivest, S. Regulation of innate immune responses in the brain. *Nature Rev. Immunol.* **9,** 429–439 (2009).
17. Saijo, K., Collier, J. G., Li, A. C., Katzenellenbogen, J. A. & Glass, C. K. An ADIOL-ERβ-CtBP transrepression pathway negatively regulates microglia-mediated inflammation. *Cell* **145,** 584–595 (2011).
18. Saijo, K., Crotti, A. & Glass, C. K. Nuclear receptors, inflammation, and neurodegenerative diseases. *Adv. Immunol.* **106,** 21–59 (2010).
19. Brady, J. P. *et al.* αB-crystallin in lens development and muscle integrity: a gene knockout approach. *Invest. Ophthalmol. Vis. Sci.* **42,** 2924–2934 (2001).
20. Xu, M. *et al.* Dopamine D3 receptor mutant mice exhibit increased behavioral sensitivity to concurrent stimulation of D1 and D2 receptors. *Neuron* **19,** 837–848 (1997).
21. Casper, K. B., Jones, K. & McCarthy, K. D. Characterization of astrocyte-specific conditional knockouts. *Genesis* **45,** 292–299 (2007).
22. Cai, L. *et al.* Ethanol-induced neurodegeneration in NRSF/REST neuronal conditional knockout mice. *Neuroscience* **181,** 196–205 (2011).

Supplementary Information is available in the online version of the paper.

Acknowledgements We thank B. Zhang and Y. J. Yan for technical assistance; L. Zhu for technical support in DNA microarray analysis; the Optical Imaging Center of ION and the Cell Biology Analysis Center of IBCB for technical support in confocal microscopy; T. L. Hagemann for providing the CRYAB construct; R. Quinlan for anti-CRYAB

antibodies, Y. Q. Ding for providing the *Drd1* and *Drd2* gene null mice; we also thank Shanghai Research Center for Model Organisms for creating *Drd2*-floxed mice. This work was supported by grants from the Chinese Academy of Sciences, National Basic Research Program of China (nos 2011CBA00408 and 2011CB504102), Natural Science Foundation of China (nos 31021063 and 31123002), and Shanghai Metropolitan Fund for Research and Development.

Author Contributions W.S., S.-z.Z. conducted most of the *in vivo* and *in vitro* experiments and the data analysis, M.T., Z.Z. prepared cell cultures, Y.-q.Y. and Y.-j.L. contributed to cell cultures; X.-h.Z. and Q.-b.Z. contributed to pilot experiments. Y.-q.Y. and Y.-y.H. contributed to genotyping; E.W. provided CRYAB mutant mice; T.C, S.-b.L. and M.X. provided *Drd3* mutant mice; J.-n.Z., G.H. provided pathological samples and/or advice and J.-w.Z. supervised the project and wrote the manuscript.

Author Information All original microarray data have been deposited in the NCBI Gene Expression Omnibus under accession number GSE41638. Reprints and permissions information is available at www.nature.com/reprints. The authors declare no competing financial interests. Readers are welcome to comment on the online version of the paper. Correspondence and requests for materials should be addressed to J.-w.Z. (jwzhou@ion.ac.cn).

METHODS

Animals. Adult or neonatal C57BL/6 mice were from Shanghai Laboratory Animal Center, Chinese Academy of Sciences. *Drd2* (B6.129S2-*Drd2*^{tm1Low}/J)[23], *Drd1* (B6.129S4-*Drd1a*^{tm1Jcd}/J)[24] heterozygous mice and *Cryab* transgenic mice (FVB-Tg(GFAP-CRYAB)141.6Mes/J) were purchased from the Jackson Laboratory (USA). *Drd2*$^{-/-}$ mice in a C57BL/6 (inbred) genetic background generated by 10 backcrosses were used in the entire study. *Drd2*-floxed mice were created by the Shanghai Research Center for Model Organisms. Briefly, the floxed *Drd2* allele was generated by introduction of *loxP* sites flanking the coding region of exon 2 of the *Drd2* locus into the mouse genome. Recombinant embryonic stem cells were injected into C57BL/6 blastocysts to produce chimaeras which were then crossed to C57BL/6 mice to produce mice heterozygous for the floxed *Drd2* allele (*Drd2*$^{flox/+}$). *Cryab* and *Drd3* mutant mice in the 129/Sv genetic background used in this study were characterized previously[19,20,25]. Human glial fibrillary acidic protein promoter (hGFAP)-Cre transgenic mice in a C57BL/6 genetic background, which was originally derived from FVB-Tg(GFAP-Cre)25Mes/J (Jackson Laboratory), were gifts from S. M. Duan. Mice harbouring a TAM-inducible Cre recombinase transgene driven by the hGFAP promoter (hGFAP-CreER^{T2}) in a C57BL/6 genetic background were provided by K. D. McCarthy[21]. Neuron-specific enolase (NSE-Cre) transgenic mice in a C57BL/6 genetic background were gifts from J. Fei. Characterization and genotyping of these mice were described previously[22]. They were maintained on a 12 h light/dark cycle at 23 °C with food and water available *ad libitum*. All procedures performed were approved by the Institutional Animal Care and Use Committee and were in accordance with the US National Institutes of Health Guide for the Care and Use of Laboratory Animals.

Tamoxifen treatments. Tamoxifen (TAM, Sigma-Aldrich) was made freshly by dissolving in 95% sunflower seed oil/5% ethanol solution by bath sonication for 20–30 min at room temperature with intermittent vortexing. Final concentration of TAM was 10 mg ml^{-1}. Two-month-old mice were injected intraperitoneally with 40–50 mg kg^{-1} with three cycles of TAM treatment at 1-month intervals. Each cycle is consisted of daily injection for 5 consecutive days. The animals were killed at age of 5 months.

Western blot analysis and quantification. Western blotting was performed as described previously[26]. The following primary antibodies were used: rabbit anti-CRYAB polyclonal antibody (pAb) (1:2,000; Stressgen); rabbit anti-IBA1 pAb (1:500; WAKO); mouse anti-GFAP monoclonal antibody (mAb) (1:1,000; Sigma-Aldrich); mouse anti-β-actin mAb (1:5,000; Sigma-Aldrich); rabbit anti-IL-1β pAb (1:1,000; Abcam); mouse anti-CD68 mAb (1:1,000; Abcam); rabbit anti-Nurr1 pAb (1:2,000; Santa Cruz Biotechnology); rabbit anti-phospho-JNK pAb (1:1,000; Cell Signaling); rabbit anti-p65 pAb (1:1,000; Santa Cruz Biotechnology); rabbit anti-phospho-p38 pAb (1:1,000; Cell Signaling); rabbit anti-phospho-ERK1/2 or ERK1/2 pAb (1:1,000; Cell Signaling); rabbit anti-phospho-AKT(Ser 473) or AKT pAb (1:1,000; Cell Signaling); rabbit anti-phospho-GSK3β(Ser 9) or phospho-GSK3β(Ser 216) or GSK3β pAb (1:1,000; Cell Signaling); rabbit anti-β-arrestin 2 pAb (1:1,000; Santa Cruz Biotechnology). The membrane was washed and incubated for 1 h at room temperature with the corresponding secondary antibodies: horseradish peroxidase (HRP)-conjugated goat anti-rabbit IgG (1:10,000; Jackson ImmunoResearch Laboratories); HRP-conjugated goat anti-mouse IgG (1:10,000; Jackson ImmunoResearch Laboratories). Peroxidase activity was detected with SuperSignal WestPico chemiluminescent substrate (Pierce Biotechnology) and visualized and digitized with ImageQuant (LAS-4000). Optical densities of bands were analysed by using ImageReader software (Fujifilm). Protein levels, quantified by computer analysis as the ratio between each immunoreactive band and the levels of β-actin, were expressed as a percentage of vehicle-treated control.

Immunofluorescence, confocal microscopy and image analysis. Sections or fixed cell cultures were incubated with one primary antibody followed by incubation with secondary antibody conjugated with either Alexa488 or Alexa555. The same sections were then incubated with another primary antibody, followed by incubation with the appropriate secondary antibody. Sections were imaged using either a cooled CCD (DP72, Olympus) on a microscope (BX51; Olympus) or a laser confocal microscope (Leica). Data were obtained and processed using Adobe Photoshop 7.0 software (Adobe Systems). In some cases, immunosignals were visualized by using 3,3-diaminobenzidine (Sigma-Aldrich).

The following primary antibodies were used: rabbit anti-tyrosine hydroxylase pAb (1:500; Chemicon); mouse anti-CRYAB mAb (2D2B6, 1:200; Santa Cruz Biotechnology or 1: 50, a gift from R. Quinlan); rabbit anti-IBA1 pAb (1:500; WAKO); rabbit anti-GFAP pAb (1:800; DAKO); mouse anti-GFAP mAb (1:1,000, Sigma-Aldrich); mouse anti-Cre (1:500, Millipore); mouse anti-tyrosine hydroxylase mAb (1:500; Chemicon).

Cell counting. The number of tyrosine-hydroxylase-positive cells was quantified in adult *Drd2*$^{-/-}$ mutants and their littermates in brain cryosections with typical morphology of the substantia nigra, as described previously[27]. Four series of cryosections were collected and every fourth section (12 μm) was used for quantification of tyrosine-hydroxylase-positive neurons. The number of GFAP^{+} or IBA1^{+} cells was quantified using a similar approach. Numbers of tyrosine-hydroxylase-positive neurons in the ventral mesencephalic (VM) cultures were counted in each well.

Intensity analysis. Average intensities of tyrosine hydroxylase, GFAP or IBA1 were calculated using ImageJ by sampling a 28 × 28 pixel area, in the substantia nigra and striatum, in 40 images taken from 4–8 consecutive sections. Values are reported as average intensity above background ± s.e.m.

Primary astrocytic culture and transfection. Astrocytes were prepared from the striatum of Sprague–Dawley rats or *Drd2*-deficient and wild-type C57BL/6 mice at P0, as described previously[28]. The neonatal striatum were trypsinized and dissociated and cells were plated at density of 5 × 10^{7} cells per 75 cm^{2} flask (Corning) in DMEM/Ham's F12 medium containing 10% FBS (in some cases, 0.5% FBS was used). Culture media were changed 24 h later to complete medium and subsequently twice a week. Cultures were shaken to remove the top layer of cells sitting over the astroglial monolayer to yield mainly type-I astrocytes with a flat morphology between day 5 and 7. Before experimental treatments, astrocytic cultures were passaged once. Cells were allowed to reach 90% confluence. Cultures were transfected using a Nucleofector device (Amaxa) with the indicated plasmids or treated with compounds at various concentrations for the indicated incubation times. Untreated cells were included as controls in all experiments.

Primary microglia culture. Neonatal mice, age 1–3 days, were used for the microglia isolation. Microglial cultures were prepared as described previously[29] with a few modifications. Briefly, the neonatal brain were trypsinized and dissociated and cells were plated in a six-well-plate at a density of 5 × 10^{4} cells cm^{-2} (Corning) in DMEM/Ham's F12 medium containing 10% FBS, penicillin and streptomycin at 37 °C in humidified 5% CO_2/95% air. Culture media were changed twice a week. Cells were allowed to reach 90% confluence. At day 9 *in vitro*, cultures were replated after trypsinization. At day 20 *in vitro*, cultures were mildly trypsinized with trypsin solution (0.07% trypsin in DMEM/Ham's F12) at 37 °C for 15–20 min. Floating cells (astrocytes and dead cells) were removed by rinsing cultures with D-Hanks' solution. The resulting enriched microglial cultures were maintained in DMEM/Ham's F12 complete medium containing 10% heat-inactivated FBS, penicillin and streptomycin until use. The purity (>99%) of these cultures was confirmed by IBA1 immunocytochemistry.

Preparation of conditioned medium. Postnatal striatal *Drd2*-null and wild-type microglia were allowed to grow to 90% confluence and treated with LPS (10 ng ml^{-1}) for 2 h[11]. The conditioned medium was collected 24 h following washing of the culture. The conditioned medium was centrifuged before use.

Mesencephalic neuronal culture. Primary VM neuronal cultures were prepared as described previously[30]. Briefly, fetuses obtained from pregnant rats on the 14th gestational day (E14, where E0 is the day of the vaginal plug) were used for preparation of VM neuronal cultures. The animals were killed with an overdose of pentobarbital sodium and the VM tissues were collected and digested with trypsin. Cell suspension was plated onto poly-L-lysine-coated 96-well plates at a density of 10^{5} cells per cm^{2} in DMEM/Ham's F12 medium (Invitrogen) containing 10% fetal bovine serum (Invitrogen). Cells were maintained at 37 °C in a 95% air/5% CO_2 humidified atmosphere for 3 h, and the cells were then switched to Neurobasal medium with 2% B27 supplement (Invitrogen).

Isolation of total RNA and Affymetrix microarray analysis. Isolation of total RNA and Affymetrix microarray analysis were performed as described previously[31]. Briefly, the striatum of 2-month-old male mice were homogenized in TRIzol reagent (Invitrogen). Total RNA was purified and complementary DNA was synthesized. The complementary RNA was prepared and biotin-labelled. Twenty micrograms of fragmented cRNA were hybridized for 16 h at 45 °C to a Mouse 430 2.0 array (Affymetrix). All RNA samples were subjected to RNA quality control by inspection on an agarose gel and measurement of 260/280 nm absorbance ratios. Array hybridization was performed following the manufacturer's protocol and the arrays were scanned using a laser confocal microscope (Affymetrix). The array was repeated twice with different batches of sample. All original microarray data have been deposited in the NCBI Gene Expression Omnibus under accession number GSE41638.

Microarray data analysis. Primary analysis was performed using Affymetrix Genechip Operating System 1.2 (GCOS1.2) software, as described previously[31], to select all of the probe sets that scored as 'present' in the control sample. The signal strengths of those probe sets were compared between *Drd2* KO and wild-type counterparts to identify any probe sets that showed increased or reduced expression in the KO sample for more than twofold compared with wild-type mice. Supplementary Table 1 showed the list of differentially expressed annotated genes and predicted genes identified using statistical analysis with Student's *t*-test, in combination with Benjamini–Hochberg (BH) multiple test correction.

***Cryab* knockdown.** Knocking down *Cryab* (GenBank accession number NC_000011) was performed as described previously[32]. Mouse primary astrocytes were seeded 2×10^5 in six-well tissue culture dishes 36 h before transfection with small interfering RNA (siRNA) targeting *Cryab* or control siRNA (Jima) using Lipofectamine 2000 (Invitrogen) according to the manufacturer's protocol. siRNA duplexes used were: sense: r(GGCCCAAAUUAUCAAGCUA)dTdT; antisense: r(UAGCUUGAUAAUUUGGGCC)dTdG; non-silencing control siRNA: sense: r(UUCUCCGAACGUGUCACGU)dTdT; and antisense: r(ACGUGACACG UUCGGAGAA) dTdT. At 72 h after transfection, cells were collected for western blot or qPCR analysis.

***In vivo* experimental treatments.** Adult mice were administered three intraperitoneal injections of 2 or 5 mg kg^{-1} quinpirole (Sigma-Aldrich, lot number 096K4603), or 0.5 or 1 mg kg^{-1} spiperone (Sigma-Aldrich), or vehicle (saline) at 8-h intervals before and after MPTP injection (Supplementary Fig. 17a). Mice were given intraperitoneal injections of l-methyl-4-phenyl-l,2,3,6-tetrahydropypridine (MPTP; 20 mg kg^{-1}) administered four times at 2 h intervals as described previously[15], and the total dose per mouse was 80 mg kg^{-1}. In some cases, mice received subacute MPTP administration. MPTP was given at 30 mg kg^{-1} for four consecutive days and left for 3 days. At day 7 post-injection, the animals were killed by rapid decapitation, and the striatum and VM were dissected and processed for western blot or qPCR analysis. In some cases, animals were perfused with 4% paraformaldehyde in 0.1 M phosphate buffer (pH 7.4) and coronal cryo-sections at a thickness of 25 μm were prepared for immunohistochemistry.

In order to test whether a DRD2 agonist exerts suppressive effect on inflammatory response in mice with 129/Sv genetic background that are known to be relatively insensitive to MPTP, animals were perfused in the striatum unilaterally with neurotoxin 6-hydroxydopamine as described previously[33]. Lesion of the nigrostriatal pathway was determined using tyrosine hydroxylase immunostaining.

RNA isolation and quantitative PCR. Brain tissue was homogenized in TRIzol reagent (Invitrogen). cDNA was synthesized from 1 μg of extracted total RNA using M-MLV Reverse Transcriptase kit (Invitrogen) according to the manufacturer's protocol. Quantitative PCR was performed with SYBR-Green premix Ex *Taq* (Takara) and detected by a Real Time PCR System (Roche LightCycler 480 or Rotorgene 6000). β-actin was used as an internal control gene. qPCR primers were designed using Primer Picking Program and their sequences were as follows:

Catalase, forward, 5′-GCATCGAGCCCAGCCCTGAC-3′, reverse, 5′-TTGG GGGCACCACCCTGGTT-3′; *COX-2*, forward, 5′-CCCTGCTGCCCGAC ACCTTC-3′, reverse, 5′-CCAGCAACCCGGCCAGCAAT-3′; *Cryab*, forward, 5′-GCACGAAGAACGCCAGGACGA-3′, reverse, 5′-GAATGGTGCGCTCA GGGCCA-3′; *IL-1β*, forward, 5′-TGCAGCTGGAGAGTGTGGATCCC-3′, reverse, 5′-TGTGCTCTGCTTGTGAGGTGCTG-3′; *IL-2*, forward, 5′-CGCAC CCACTTCAAGCTCCACTTC-3′, reverse, 5′-ATTCTGTGGCCTGCTTGG GCAAG-3′; *IL-6*, forward, 5′-GGTGCCCTGCCAGTATTCTC-3′, reverse, 5′-GGCTCCCAACACAGGATGA-3′; *IL-12β*, forward, 5′-TGGTTTGCCA TCGTTTTGCTG-3′, reverse, 5′-ACAGGTGAGGTTCACTGTTTCT-3′; IFN-γ, forward, 5′-GGCTGTTACTGCCACGGCACA-3′, reverse, 5′-CACCATCCTT TTGCCAGTTCCTCCA-3′; inducible NO synthase (iNOS), forward, 5′-GCTGCCTTCCTGCTGTCGCA-3′, reverse, 5′-CCTGACCATCTCGGGTGCG G-3′; *TNF-α*, forward, 5′-ACTTCGGGGTGATCGGTCCCC-3′, reverse, 5′-TGGTTTGCTACGACGTGGGCTAC-3′; *Hsp25* (also known as *Hspb1*), forward, 5′-CGGTGCTTCACCCGGAAATA-3′, reverse, 5′-AGGGGATAGGGAAAGA GGACA-3′; *Gpx1*, forward, 5′-TCGGACACCAGGAGAATGGCA-3′, reverse, 5′-GAGCGCAGTGGGGTCGTCAC-3′; *Gpx3*, forward, 5′-CCTTTTAAGCAGT ATGCAGGCA-3′, reverse, 5′-CAAGCCAAATGGCCCAAGTT-3′; β-actin, forward, 5′-GAGATTACTGCCCTGGCTCCTA-3′, reverse, 5′-TCATCGTA CTCCTGCTTGCTGAT-3′. Following PCR amplification, a first derivative melting-curve analysis was performed to confirm the specificity of the PCR. The relative fold difference in mRNA between samples was calculated by comparing the threshold cycle (C_t) at which product initially appeared above background according to: $2^{-(\Delta Ct)}$, where ΔC_t is the difference between control group and a treatment group.

Statistical analysis. Statistical analysis was performed using GraphPad software (GraphPad Prism v5.0; GraphPad Software). Data presented as mean ± s.e.m. were submitted to one/two-way ANOVA followed by either Dunnet test or Student–Newman–Keul's test (as a post hoc test). $P < 0.05$ was considered as significant in statistics.

23. Kelly, M. A. *et al.* Pituitary lactotroph hyperplasia and chronic hyperprolactinemia in dopamine D2 receptor-deficient mice. *Neuron* **19,** 103–113 (1997).
24. Drago, J. *et al.* Altered striatal function in a mutant mouse lacking D1A dopamine receptors. *Proc. Natl Acad. Sci. USA* **91,** 12564–12568 (1994).
25. Ousman, S. S. *et al.* Protective and therapeutic role for αB-crystallin in autoimmune demyelination. *Nature* **448,** 474–479 (2007).
26. Li, A. *et al.* Apomorphine-induced activation of dopamine receptors modulates FGF-2 expression in astrocytic cultures and promotes survival of dopaminergic neurons. *FASEB J.* **20,** 1263–1265 (2006).
27. Sauer, H., Rosenblad, C. & Bjorklund, A. Glial cell line-derived neurotrophic factor but not transforming growth factor beta 3 prevents delayed degeneration of nigral dopaminergic neurons following striatal 6-hydroxydopamine lesion. *Proc. Natl Acad. Sci. USA* **92,** 8935–8939 (1995).
28. Menet, V. *et al.* Inactivation of the glial fibrillary acidic protein gene, but not that of vimentin, improves neuronal survival and neurite growth by modifying adhesion molecule expression. *J. Neurosci.* **21,** 6147–6158 (2001).
29. Saura, J., Tusell, J. M. & Serratosa, J. High-yield isolation of murine microglia by mild trypsinization. *Glia* **44,** 183–189 (2003).
30. Guo, H. *et al.* Apomorphine induces trophic factors that support fetal rat mesencephalic dopaminergic neurons in cultures. *Eur. J. Neurosci.* **16,** 1861–1870 (2002).
31. Zhou, Q., Li, J., Wang, H., Yin, Y. & Zhou, J. Identification of nigral dopaminergic neuron-enriched genes in adult rats. *Neurobiol. Aging* **32,** 313–326 (2011).
32. Dimberg, A. *et al.* αB-crystallin promotes tumor angiogenesis by increasing vascular survival during tube morphogenesis. *Blood* **111,** 2015–2023 (2008).
33. Sauer, H. & Oertel, W. H. Progressive degeneration of nigrostriatal dopamine neurons following intrastriatal terminal lesions with 6-hydroxydopamine: A combined retrograde tracing and immunocytochemical study in the rat. *Neuroscience* **59,** 401–415 (1994).